



Operating control strategies and dimensioning of photovoltaic-powered reverse osmosis desalination plants without batteries

A. Schies*, J. Went, C. Heidtmann, M. Eisele, F. Kroemke, H. Schmoch, M. Vetter

Fraunhofer Institute for Solar Energy Systems, Heidenhofstr. 2, 79110 Freiburg, Germany

Tel. +4976145885460; Fax +4976145885240; email: alexander.schies@ise.fraunhofer.de, joachim.went@ise.fraunhofer.de

Received 8 May 2009; accepted 16 May 2010

ABSTRACT

Small photovoltaic reverse osmosis systems (PV-RO) without batteries are not driven constantly at their operating point, but are tracked to the solar power offered. Because of this intermittent and dynamic operation, high requirements for the operating control strategies must be satisfied. A PV-RO system has been modelled in the Dymola simulation environment. This system minimizes the specific energy consumption (SEC) and accordingly distributes the incoming PV power to the different pumps in the PV-RO system. The operating control strategy also accounts for the requirements stipulated by the membrane producer. To obtain the required amount of permeate every day of the year, a tool has been developed especially for dimensioning the PV generator for the PV-RO system under the local boundary conditions.

1. Introduction

Desalination of brackish water and seawater in decentralized small scale installations presents an interesting and cost effective solution in many regions with water shortage. Because of the high energy demand for desalination technology and the generally good coincidence of regional water demand and solar irradiation, promising research activities are already being carried out concerning solar driven reverse osmosis plants [1–8]. There is an overview of plants and field tests in the “Compendium on Autonomous Desalination Units Using Renewable Energy Sources” [9] which was developed during the EU project “ADU-RES”. Most of them are solar battery or wind battery systems driven at a steady state operating point. To avoid the disadvantages of the short life times of batteries and to reduce the lifecycle costs, the next generation of PV driven desalination plants have been

planned without batteries, and use the desalinated water as a kind of storage [8,10].

In an ongoing project at Fraunhofer ISE, small, autonomous seawater desalination plants without batteries for use in decentralized areas in the scale of 0.06–1 m³/h and 0.3–5 m³/d are being developed.

This article presents an operating control strategy developed in the Dymola simulation environment using the modelling language Modelica and the dimensioning of PV driven desalination plants.

2. Objectives

This paper shows the operability of the dynamic RO process in a direct coupled PV-RO system without the use of batteries in a simulation. Special requirements related to the operating control strategies have to be considered here. The system setup is simulated in order to implement an operating control strategy. An overview of the modelled system setup is given in Fig. 1. The modelling of the system is described based

*Corresponding author

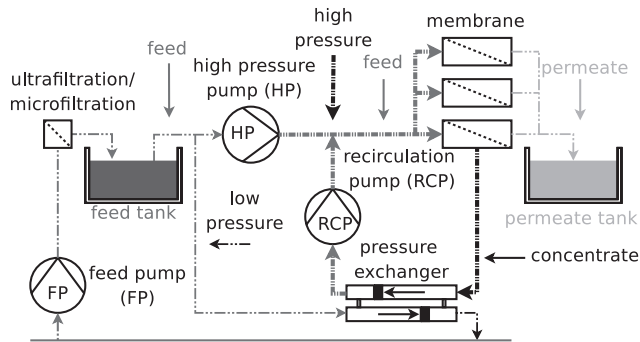


Fig. 1. Diagram of the PV-RO plant. The feed pump conveys water through the ultrafiltration and microfiltration into the feed tank. The high pressure pump and the energy recovery unit feed the high pressure circuit to desalinate the feed water. Each of the three RO membranes can be switched on dependent on the PV power available.

on the example of the membrane model. Furthermore, this paper presents a method for dimensioning PV generators for PV-RO systems.

3. Plant design and simulation

In comparison to RO processes driven at their nominal operating point, direct coupled PV-RO plants have additional requirements

- good part load behavior,
- flexible control of partial processes,
- gentle start-up and shutdown behavior.

In order to choose the system concept, an analysis method was developed in [11]. The most promising concept is presented in Fig. 1.

Seawater is pumped into the elevated feed tank by a pump (feed pump, FP). The high pressure pump and the energy recovery unit are supplied by the feed tank. The high pressure pump (HP) provides the necessary pressure for the RO process. The energy recovery unit in the form of a pressure exchanger uses the high pressure at the concentrate exit of the membrane and transmits it to fresh feed water at the entrance of the recirculation pump in the high pressure circuit. The recirculation pump (RCP) compensates the pressure loss of the membrane and the pressure exchanger process, and in addition delivers high pressure feed water to the entrance of the RO membrane. The pressure exchanger is refilled with fresh feed water through hydrostatic pressure from the feed tank. Fresh water is stored in the permeate tank. There are three parallel RO membranes which can be switched on according to available PV power.

Models of all components were developed for this PV driven RO desalination plant in the Dymola

simulation environment on the basis of the object orientated modelling language, Modelica. The models of the different components are connected by interfaces. Flow and potential values are exchanged via these interfaces. For the hydraulic model, the flow values are mass flow, enthalpy flow and salt mass flow, whereas the potential values are pressure, enthalpy and salt concentration. All models are realized bidirectionally, so the mass flow is possible in two directions. It is possible to access further variables defined in the fluid model such as density or viscosity in the different models. Furthermore, the basic fluid dynamics and hydraulic equations are the three conservation equations of mass, impulse and energy. For a fluid consisting of two components (binary), as simplified here for saltwater, an additional fourth conservation equation is introduced for the mass of salt. In such conservation equations, the changes of stocks of a physical value in a defined volume dependent on the flows into or out of the volumes are described. A one-dimensional description is adequate for technical simulation (one-dimensional fluid element theory [12,13]). A dynamic simulation is possible through this set up, in which the models influence each other.

Water is simulated as a binary fluid of water and salt and is described with different complexities of hydraulic equations. There are two kinds of pump models modelled; firstly a positive displacement pump modelled with mechanical and hydraulic equations. Secondly there are sets of characteristic curves to describe the pump's behavior. The microfiltration and ultrafiltration is modelled as a closing valve to simulate the increasing filter resistance because of layer formation. A valve is used because water is modelled as a binary fluid and no particulate contamination is considered. The tanks are open basins which can be used to extract water. The pipes are simulated with friction. As with all hydraulic components, the pressure exchanger is modelled with fluid dynamics and hydraulic equations.

As an example, the model of the RO membrane is described in detail. The principle is a pressure vessel with three connectors as shown in Fig. 2. The module contains two control volumes, (A) with saltwater, and (B) with permeate. The osmotic pressure is the most important factor effecting the permeate production. The osmotic pressure is defined as:

$$\pi^i = \frac{-\Re \cdot T}{V^i} \cdot \ln(a^i), \quad (1)$$

\Re describes the gas constant, T the absolute temperature, V^i the volume and a^i the activity of the component i . For $\Delta\pi = \pi_A - \pi_B$ this implies:

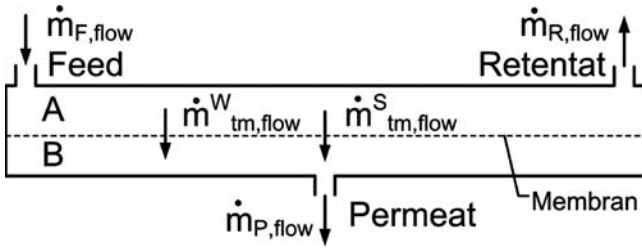


Fig. 2. Diagram of RO module with most important mass flows. \dot{m}_F is the mass flow of the feed water, \dot{m}_R is the concentrate mass flow and \dot{m}_P is the permeate mass flow. A and B are control volumes. The mass flow through the membrane is subscripted with tm (transmembrane), so \dot{m}_{tm}^W is the water mass flow and \dot{m}_{tm}^S the salt mass flow through the membrane.

$$\Delta\pi^i = \frac{-\mathfrak{R} \cdot T}{V^i} \cdot \ln\left(\frac{a_A^i}{a_B^i}\right). \quad (2)$$

Different temperatures within the membrane and different molar volumes were neglected. For constant water concentration over the membrane layer, constant water diffusion coefficients in the membrane, constant pressure in the membrane and chemical balance at phase boundaries, the area specific transmembrane water mass flow ($i = W = \text{water}$) is calculated according to [14]:

$$\frac{\partial \dot{m}_{tm}^W}{\partial A} = M^W \cdot \underbrace{\frac{\bar{c}_M^W \cdot D_{M,0}^W}{\mathfrak{R} \cdot T \cdot \delta_M} \cdot V_{mol}^W \cdot [\Delta p - \Delta\pi^W]}_{\Delta\mu^W} \cdot \frac{\partial \dot{n}^W}{\partial A}. \quad (3)$$

In this case \bar{c}_M^W in [mol/L] is the constant water concentration in the membrane, $D_{M,0}^W$ is the water diffusion coefficient in the membrane, δ_M is the boundary layer thickness of the active membrane layer, \dot{n}^W is the molar flow of water through the membrane and M^W is the molar mass of water. With consistency of all parameters over the membrane area, A_M (homogeneous circumstances in Volume A and B) is the mass flow integrated over the area:

$$\dot{m}_{tm}^W = A_M \cdot M^W \cdot \underbrace{\frac{\bar{c}_M^W \cdot D_{M,0}^W}{\mathfrak{R} \cdot T \cdot \delta_M} \cdot V_{mol}^W}_{\sigma_M^W} \cdot [\Delta p - \Delta\pi^W], \quad (4)$$

σ_M^W is the area specific permeability of the membrane for water. As far as salt is concerned, in [14] it is shown that the pressure gradient Δp has nearly no influence

on the transmembrane salt flow and can be neglected. This implies according to [14]:

$$\dot{m}_{tm}^S = A_M \cdot M^S \cdot \underbrace{\frac{c_M^{ges} \cdot D_{M,0}^S \cdot \gamma_{AB}^S}{\bar{\gamma}_M^S \cdot \delta_M}}_{\sigma_M^S} \cdot [x_A^S - x_B^S]. \quad (5)$$

Here, σ_M^S is the area specific permeability of the membrane for salt. The detailed calculation of the membrane permeability for salt and water is not made in this model, but the resulting values were directly given as parameters. The values are taken out of datasheets or empirical calculations [14]. In addition, a temperature and pressure difference dependency of the permeability will be introduced [14, 5]:

$$\begin{aligned} \sigma_M^W &= \sigma_{M,0}^W(p, T_M) = \sigma_{M,0}^W \cdot \exp\left(\alpha_p \cdot \frac{p_M - p_0}{p_0}\right) \\ &\quad \cdot \exp\left(\alpha_T \cdot \frac{T_M \cdot T_0}{T_0}\right) \\ \sigma_M^S &= \sigma_{M,0}^S(p, T_M) = \sigma_{M,0}^S \cdot \exp\left(\beta_p \cdot \frac{p_M - p_0}{p_0}\right) \\ &\quad \cdot \exp\left(\beta_T \cdot \frac{T_M \cdot T_0}{T_0}\right). \end{aligned} \quad (6)$$

[14] advises $\alpha_p = -0.005 \dots -0.003$, $\alpha_T = 7,08$, $\beta_p \approx 0$, $\beta_T = 3.0$. [15] and [16] advise similar values.

The electrical part comprehends a solar cell in the form of a two diode model and also a module with characteristic curves depending on temperature and irradiation. A three phase inverter with an integrated control mechanism is required to feed the asynchronous motor. The asynchronous motor is modelled with electrical equations, but also one model is integrated in the characteristic curve of the different pumps.

This detailed modelling is an important base for developing operating control strategies. Using the simulation, it is possible to obtain information on permeate, concentrate and feed flows, salt content of the feed and permeate, temperature and energy consumption of the system.

2.1. Demands on the operating system

Unlike known PV-RO systems, the power input of the hydraulic part in this work is controlled depending on the available solar power. Therefore the operating point is always dependent on the solar power. Despite this intermittent operation, the operation requirements of the membrane producer always have to be kept within range.

The requirements for the operating control strategies are:

- optimal usage of the incoming PV power,
- conductivity quality of desalinated water,
- low maintenance and material protection to guarantee a long lifetime,
- abdication of chemical additives (if possible),
- target quantity of desalinated water.

2.2. Solution statement for operating control strategy

By introducing the feed tank into the system, the conveying process and the desalinating process are divided into two independent actions and can be controlled independently. In this way, the energy can be shared to drive the pumps consistently at their best point of operation with the specific available solar power. To ensure that the same average amount of water is pumped into the feed tank as is withdrawn for the desalination process, the dimensions of pumps and PV generators must be chosen accurately.

The PV-RO system is controlled via the optimum recovery rate and feed pressure to achieve the highest permeate output per energy. The boundary conditions of start-up and shutdown must be taken into consideration. Fig. 3 shows the simplified operating control strategy.

The incoming power is the PV power in the maximum power point. First the power needed for measurements is drawn off. Then the power for controlling the recirculation pump (RCP) to the optimum recovery ratio is subtracted. The rest of the power is divided between the high pressure pump (HP) and the feed pump (FP) in such a way that each pump works at the optimum operating point for each specific irradiation condition. Furthermore, the control algorithm gives set points of pressure (HP) and maximum power (FP), leading to a power demand. Depending on the weather conditions, the demand is satisfied by the power distribution to the HP and FP or not. If the demand is satisfied, then excess power is left. If the power demand is not satisfied, the maximum available

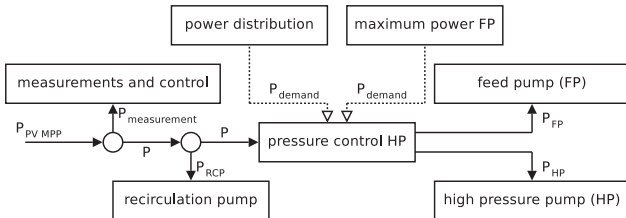


Fig. 3. Simplified operation control strategy. After subtracting the power for measurements, control and the recirculation pump, the remaining power is distributed according to the optimum operating point to the high pressure pump and the feed pump.

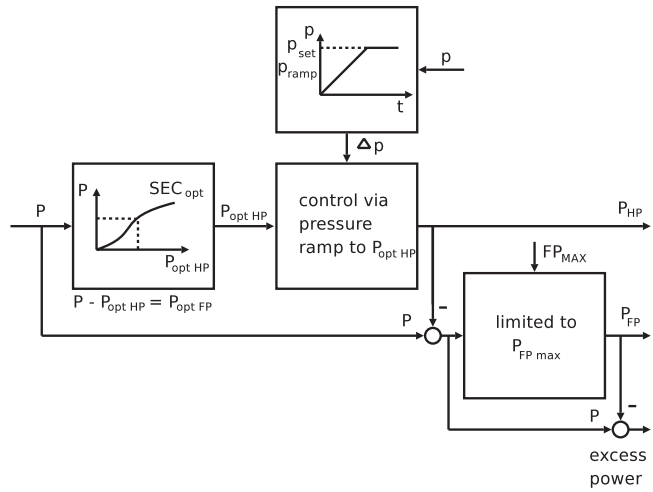


Fig. 4. Power distribution of the optimized control: The algorithm SEC_{opt} gives the power distributed to the HP, $P_{opt\ HP}$. P minus $P_{opt\ HP}$ is equal $P_{opt\ FP}$. In the next step the P_{HP} is controlled via the pressure ramp to $P_{opt\ HP}$. P_{HP} minus the available power P gives P_{FP} . The P_{FP} is limited to $P_{FP\ max}$. If P minus P_{HP} and P_{FP} is bigger than zero excess power is left (unused). If there is no change in available power, the P_{HP} and P_{FP} will get to $P_{opt\ HP}$ and $P_{opt\ FP}$.

power (maximum power point power) is distributed and a droop is accepted.

Fig. 4 shows in detail the box “power distribution” of Fig. 3. The algorithm SEC_{opt} gives the power distributed to the HP, $P_{opt\ HP}$. A fixed ramp for the HP is defined for a gentle rise to the set pressure ($\Delta p / \Delta t$). This ramp and the set pressure are given through the membrane properties and manufacturer recommendations. In cases of a fast change of the available power, the FP can react fast to the change and the HP is driven slowly on the preset ramp to the new setpoint of optimal SEC conditions to $P_{opt\ HP}$. P_{HP} minus the available power P gives P_{FP} . The P_{FP} is limited to $P_{FP\ max}$. If P minus P_{HP} and P_{FP} is bigger than zero excess power is left. If there is no change in available power, and because P minus $P_{opt\ HP}$ is equal to $P_{opt\ FP}$, the P_{HP} and P_{FP} will get to $P_{opt\ HP}$ and $P_{opt\ FP}$.

To cover the boundary conditions such as scaling, fouling and mechanical stability, several features have been established in the operating control strategy. A minimum overflow to the membrane and an allowed maximum recovery ratio are ensured via control against scaling and fouling. There are also several flushing procedures for the ultrafiltration and the RO membrane; one each morning and evening and several after predefined time steps and pressure limits. For cleaning the ultrafiltration and RO membranes, and for keeping to the mechanical requirements, the start-up and shutdown procedures have to be carried out based

on the membrane producer’s recommendations. Before start-up of the desalination, the ultrafiltration and microfiltration must be back flushed, then the RCP starts to flush the RO membrane with low pressure seawater to prevent high flux diffusion of permeate through the membrane with harsh mechanical stress. In the next step the HP starts and increases the pressure via a ramp. For shutdown the desalination the HP is stopped, and then flushing is carried out using feed water without producing permeate in order to flush out the high salt concentration. In the next step, all valves are closed.

To avoid a feed tank emptying while the desalination is working, a special feed tank control algorithm is implemented into the operating control strategy. If the amount of water in the feed tank falls below a certain limit, the power distribution is changed to convey more water into the feed tank than is extracted. A control mechanism to avoid feed tank overflow is also implemented. If the feed tank is full, the FP conveys the same water as is extracted for desalination.

For optimal power distribution, the specific energy consumption (SEC) is minimized to find the best operating point for each pump by each specific power given from the PV generator. The SEC is the energy required to gain a specific volume of permeate.

$$\overline{SEC} = \frac{E}{V_P} \quad SEC = \frac{P}{\dot{V}_P} = \frac{P_{RCP} + P_{HP} + P_{FP}}{\dot{V}_P} \quad (7)$$

This formula takes P as power, E as energy and \dot{V} as volume flow. Because of the divided process of conveying and desalination, the SEC is:

$$SEC_{total} = SEC_{conveying} + SEC_{desalinating} = \frac{P_{FP}}{\dot{V}_{FP} \cdot \Phi} + \frac{P_{RCP} + P_{HP}}{\dot{V}_P} \quad (8)$$

As the recovery ratio for preventing scaling may not be higher than about 35% and optimum ratios in the assumed application are higher, the recovery ratio is adjusted slightly lower than 35% as constant. P_{RCP} depends on the recovery ratio. This leads to a specific distribution of power for the two pumps for the conveying and desalination processes. Fig. 5 shows the power distribution on a sunny day for permeate production of about 12 m³. Fig. 6 shows the feed tank water level on the same day.

2.3. Dimensioning of the PV generator

To dimension the PV generator for battery-less operation of a PV-RO installation, an iterative process was developed (Fig. 7). For the dimensioning of the

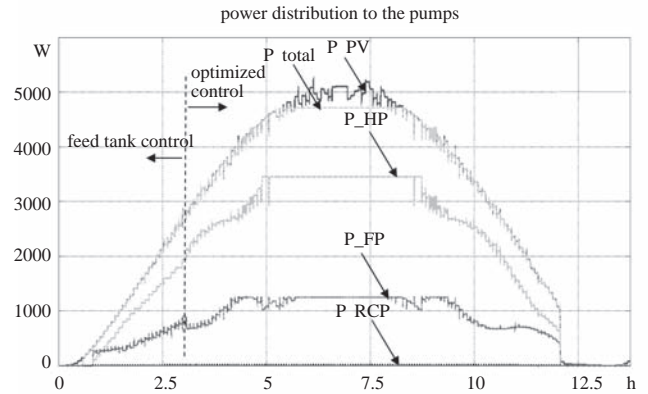


Fig. 5. This simulation with Modelica/Dymola uses a measured 6 min irradiance data from a sunny day in Freiburg Germany, the sample time for the simulation is 1 s. It shows the power distribution on a sunny day, starting at about 6 a.m. P_{PV} is the solar power, P_{total} is the power of all loads, P_{HP} is the power of the high pressure pump, the feed pump power is P_{FP} and P_{RCP} is the power of the recirculation pump. From 0 to about 3 h, the feed tank is empty and the feed tank control algorithm works; then normal power distribution algorithm starts with “optimized control”.

PV generator, the two processes of water pumping and pre-treatment and the desalination process are considered separately. Thus common dimensioning software can be used to identify suitable PV generators for the pumping and the desalination processes.

In the first step the energy consumption for the desalination process is calculated on the basis of a

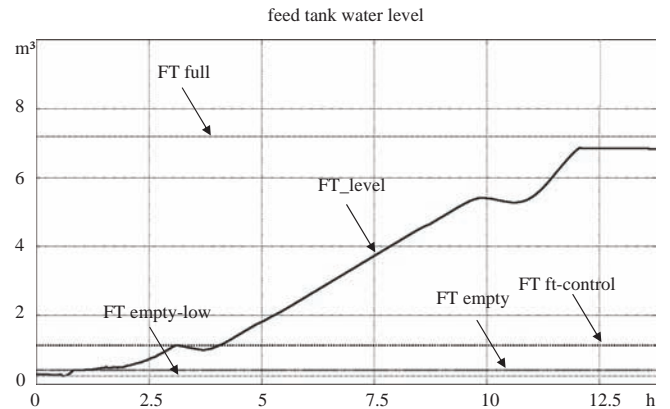


Fig. 6. This figure, simulated with Modelica/Dymola, shows the feed tank level over one day. The feed tank water level is the black line “FT_level”. The feed tank control algorithm works its way up to the intersection point of the “FT_level” and the line “FT ft-control”. If the tank level rises higher than this threshold once, the normal power distribution “optimized control” starts, until the feed tank level crosses the “FT full” or the “FT empty” line.

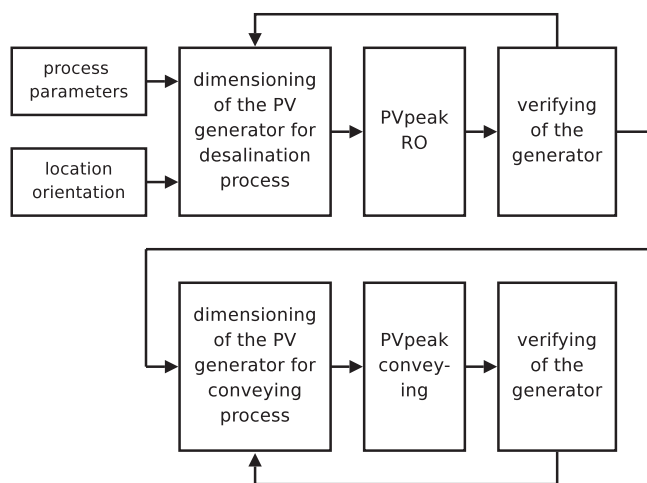


Fig. 7. Iterative dimensioning of PV generators for desalination.

stationary operation. Using this average energy demand, the required PV generator is defined with any available dimensioning software for a certain location.

In a second step, the size of the PV generator is verified by using a characteristic curve for the dynamic RO process. The operating strategy leads to a simplified characteristic curve which allows a correlation between a certain solar irradiation and certain permeate flow, taking the liquid levels of the feed and permeate tanks into consideration. The hourly electric power calculated by the dimensioning tool is used as an input value. This data and the load profile of the RO system is used to calculate the filling level of the permeate tank. An overview over a year shows critical situations where not enough water is available (Fig. 8). If the security of supply is insufficient, the permeate storage tank or the PV generator must be increased. The same

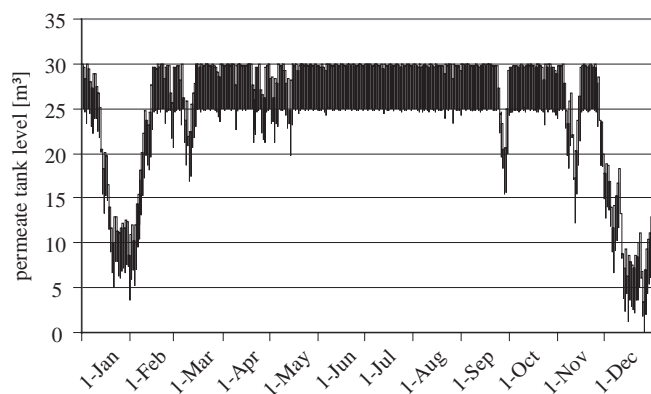


Figure 8. Yearly overview of the permeate tank level with an extraction of 5 m³ per day. The simulation is done with hourly Meteonorm irradiation data from Paphos/Cyprus.

procedure is executed for the conveying process, to check the filling level of the feed tank over the year. Fig. 8 shows the filling level of the permeate tank during one year. In this example 5 m³ are withdrawn every day. The dimensioning is realized using irradiation data for Paphos/Cyprus.

6. Discussion

The models of the solar components are validated through measured data from systems set up in the laboratories at Fraunhofer ISE in Freiburg and the out of field test. The hydraulic models are validated at a small laboratory prototype with a flowrate of about 0.4 l/h, and have yet to be validated for the bigger systems. The operating control strategy has only been tested in simulations, but there it shows a good performance, gentle variations of power distributions (Fig. 5) and therefore also gentle pressure changes. The operating control strategy can distribute the power in such a way that both independent pumps work at the optimal operating point in every irradiation situation. In this way, efficient operation of the whole system at any time is possible.

7. Conclusion

After testing and verifying the operation control algorithm at the Fraunhofer ISE laboratories, a field test for two systems of different size is to be realized. The tools developed for simulation and dimensioning can be utilised for all kinds of dynamic loads; also for brackish water, big pumping stations and irrigation. The concept of using water tanks as storage instead of electrical storage is extremely interesting. Furthermore water treatment systems may be used as shiftable loads, also for hybrid PV mini grids, for example in village electrification programs with a high proportion of PV or other renewable energy sources.

Abbreviations

FP	feed pump
HP	high pressure pum
PV	photovoltaic
PV-RO	photovoltaic reverse osmosis system
RCP	recirculation pump
RO	reverse osmosis
SEC	specific energy consumption

Symbol

A	Area
A	activity
c	concentration
D	water diffusion coefficient

F	feed
M	molar mass
\dot{m}	mass flow
\dot{n}	molar flow
P	permeate
p	pressure gradient
R	retentate, concentrate
S	salt
T	absolute temperature
T _m	transmembrane
V	volume
W	water
\bar{xyz}	Midpoint, mean value
α	coefficient
β	coefficient
Δ	delta difference
δ	boundary layer thickness of the active membrane area
μ	dynamic viscosity
π	osmotic pressure
σ	area specific permeability
\mathcal{R}	gas constant

Deep indices

A	control volume A
B	control volume B
F	Feed
P	permeate
R	retentate, concentrate
tm	transmembrane
M	membrane
P	pressure
T	temperature
RCP	recirculation pump
HP	high pressure pump
FP	feed pump

High indices

i	component (here W or S)
ges	total
S	Salt
W	Water

Acknowledgements

This work is supported in part by Pairan Elektronik GmbH, IBC Solar AG, Gather Industrie GmbH, MAT Plasmatec GmbH, Katadyn Products Inc., TBB and the

German Federal Ministry of Economics and Technology BMWi (16INO538).

References

- [1] E.S. Mohamed, et al., An experimental comparative study of the technical and economic performance of a small reverse osmosis desalination system equipped with a hydraulic energy recovery unit. *Desalination*, 194(1–3) (2006) 239–250.
- [2] E.S. Mohamed et al., The effect of hydraulic energy recovery in a small sea water reverse osmosis desalination system; experimental and economical evaluation. *Desalination; Desalination and the Environment*, 184(1–3) (2005) 241–246.
- [3] B.G. Keeper, R.D. Hembree, and F.C. Schrack, Optimized matching of solar photovoltaic power with reverse osmosis desalination. *Desalination*, 54 (1985) 89–103.
- [4] A. Al-Karaghoul, D. Renne, and L.L. Kazmerski, Technical and economic assessment of photovoltaic-driven desalination systems. *Renewable Energy*, 35(2) (2010) 323–328.
- [5] M. Thomson, M.S. Miranda, and D. Infield, A small-scale seawater reverse-osmosis system with excellent energy efficiency over a wide operating range. *Desalination*, 153(1–3) (2003) 229–236.
- [6] A. Joyce, et al., Small reverse osmosis units using PV systems for water purification in rural places. *Desalination*, 137(1–3) (2001) 39–44.
- [7] A. Bermudez-Contreras, M. Thomson, and D.G. Infield, Renewable energy powered desalination in Baja California Sur, Mexico. *Desalination; European Desalination Society and Center for Research and Technology Hellas (CERTH), Sani Resort 22 - 25 April 2007, Halkidiki, Greece, European Desalination Society and Center for Research and Technology Hellas (CERTH), Sani Resort, 2008*. 220(1–3), 431–440.
- [8] D.B. Riffel, and P.C.M. Carvalho, Small-scale photovoltaic-powered reverse osmosis plant without batteries: Design and simulation. *Desalination*, 247(1–3) (2009) 378–389.
- [9] DU-RES, Autonomous Desalination Units Using Renewable Energy Sources. 2004.
- [10] M. Thomson, Reverse-Osmosis Desalination of Seawater Powered by Photovoltaic without Batteries, 2003, Loughborough University.
- [11] J. Went et al. Energy demand for reverse osmosis concepts with energy recovery in solar driven seawater desalination units. in *Desalination for the Environment - Clean Water and Energy*. 2009. Baden-Baden, Germany.
- [12] H. Elmquist, H. Tummescheid, and M. Otter. Object orientated Modeling of Thermo-Fluid Systems. in *3rd International Modelling Conference*, 2003.
- [13] H. Oertel, M. Böhle, and I. Dohrmann, *Strömungsmechanik (Grundgleichungen, Lösungsmethoden, Softwarebeispiele)*. Vol. 4. 2006: Vieweg-Verlag.
- [14] T. Melin and R. Rautenbach, *Membranverfahren; Grundlagen der Modul- und Anlagenauslegung*. VDI-Buch., 3 (2007), 584.
- [15] H. Niemi, Modelling, simulation and optimization of ultrafiltration and reverse osmosis processes. 2000, Lappeenranta University of technology, Finland; ACTA POLYTECHNICA SCANDINAVICA, Chemical technology series No. 279.
- [16] C.M. Carvalho, Photovoltaik- und windkraftbetriebene Umkehrosmosisanlagen im Inselbetrieb. 1997, Universität-Gesamthochschule Paderborn.